LA-UR- 98-1970

Approved for public release; distribution is unlimited.

Title: CHARACTERIZATION OF PHOTOLUMINESCENT EUROPIUM DOPED YTTRIUM OXIDE THIN-FILMS PREPARED BY METALLORGANIC CHEMICAL VAPOR DEPOSITION

CONF-971201--

Author(s): J. MCKITTRICK, C.F. BACALSKI, G.A. HIRATA
UNIVERSITY OF CALIFORNIA - SAN DIEGO

K.M. HUBBARD, S.G. PATTILLO, K.V. SALAZAR AND M. TRKULA
LOS ALAMOS NATIONAL LABORATORY

Submitted to: MATERIALS RESEARCH SOCIETY PROCEEDINGS

Los Alamos
NATIONAL LABORATORY

DISCLAIMER

DISCLAIMER

Portions of this document may be illegible in electronic image products. Images are produced from the best available original document.

Characterization of Photoluminescent $(Y_{1-x}Eu_x)_2O_3$ Thin-Films Prepared by Metallorganic Chemical Vapor Deposition

J. McKittrick, C.F. Bacalski and G.A. Hirata
Dept. of Applied Mechanics and Engineering Sciences and Materials Science Program, University of California at San Diego, La Jolla, CA 92093-0411

K.M. Hubbard, S.G. Pattillo, K.V. Salazar and M. Trkula
Los Alamos National Laboratory, Materials Science and Technology Division, Los Alamos, NM 87545

Abstract

Europium doped yttrium oxide, $(Y_{1-x}Eu_x)_2O_3$, thin-films were deposited on silicon and sapphire substrates by metallorganic chemical vapor deposition (MOCVD). The films were grown in a MOCVD chamber reacting yttrium and europium tris(2,2,6,6,-tetramethyl-3,5-heptanedionates) precursors in an oxygen atmosphere at low pressures (5 Torr) and low substrate temperatures (500-700°C). The films deposited at 500°C were flat and composed of nanocrystalline regions of cubic Y_2O_3, grown in a textured [100] or [110] orientation to the substrate surface. Films deposited at 600°C developed from the flat, nanocrystalline morphology into a plate-like growth morphology oriented in the [111] with increasing deposition time. Monoclinic $Y_2O_3:Eu^{3+}$ was observed in x-ray diffraction for deposition temperatures ≥ 600°C on both (111) Si and (001) sapphire substrates This was also confirmed by the photoluminescent emission spectra.

Introduction

Photo- and cathodoluminescent thin-films have potential application in emissive flat panel displays such as field emission and plasma panel displays. Field emission flat panel displays require thinner screens that operate under lower voltages, without sacrificing brightness or contrast. Thin-films, as opposed to the traditional discreet powder screens, offer the benefit of reduced light scattering, a reduction of material waste and the potential to fabricate smaller pixel sizes to enhance resolution. Europium doped yttrium oxide, $(Y_{1-x}Eu_x)_2O_3$ (x=0.03-0.20) or $Y_2O_3:Eu^{3+}$, is a well known photo- and cathodoluminescent material used for television screens and fluorescent lighting [1]. The fluorescent emission results from the 5d→4f electronic transitions in the Eu^{3+} ion. Figure 1 shows the energy level diagram for the free Eu^{3+} ion. Since the rare earth elements in a solid are shielded by the outer 5s and 5p electrons, the free ion scheme can be used to analyze the transitions occurring in an ionic crystal. Excitation of the Eu^{3+} ion results in the promotion of the electrons into the ^5D_J manifold with emission occurring during relaxation to the ^7F_J ground state manifold.

The luminescent properties of $(Y_{1-x}Eu_x)_2O_3$ has mainly been studied as single crystals [2-6] at concentration levels of $0.01 \leq x < 0.05$. $(Y_{1-x}Eu_x)_2O_3$ is an insulator, with a band gap energy of 5.6 eV and is strongly absorbing at energies with wavelengths < 250 nm. Y_2O_3 has a cubic space group, T_h^7, containing 8 yttrium sites of C_{3i} point symmetry and 24 sites of C_2 point symmetry. The ionic radii of Y^{3+} and Eu^{3+}, 0.092 nm and 0.098 nm, respectively, are similar and the Eu^{3+} ions populate the two different site symmetries with equal probability [6]. The emission spectrum is characterized by an intense, narrow feature at 611 nm arising from the $^5D_0 \rightarrow {}^7F_2$ transition from Eu^{3+} in the C_2 site. Less intense features occurring in the 580-599 nm region arise from Eu^{3+} occupation of both the C_2 and C_{3i} sites and involve the $^5D_0 \rightarrow {}^7F_1$ transitions. Figure 2 shows a typical photoluminescent (PL) excitation and emission spectra for powders of $(Y_{1-x}Eu_x)_2O_3$, with the transitions labeled.

It has been observed there are profound microstructural influences on the PL spectra of $(Y_{1-x}Eu_x)_2O_3$ powders [7]. Small crystallite sizes, typically < 200 nm show a weak fluorescence and increase in PL intensity with an increase in crystallite size. The increase in crystallite size is usually achieved by post-synthesis, high temperature annealing (>1000°C). For very fine crystallite sizes, Eilers and Tissue [8] reported that both monoclinic $Y_2O_3:Eu^{3+}$ and Eu_2O_3 formed in nanocrystalline powders produced by gas condensation. Grytsiv et al. [9] found both cubic and monoclinic Y_2O_3 in thin films prepared by reactive rf diode sputtering. The monoclinic phase of Y_2O_3 is a high temperature phase that can be obtained in bulk by quenching under high pressure [10]. Nanocrystalline monoclinic Y_2O_3 is thought to exist under ambient conditions due to the Gibbs-Thompson effect [11]. The fluorescence spectra of the 12 nm $Y_2O_3:Eu^{3+}$ particles consist of a large feature at 625 nm and two smaller features at 615 and 619 nm, attributed to the $^5D_0 \rightarrow {}^7F_2$ transitions. Nanocrystalline Eu_2O_3 shows a similar fluorescence spectrum to that of $Y_2O_3:Eu^{3+}$, except the feature at 615 nm is split into 2 features , centered around 615 nm. In later work, it was found that the solubility of Eu^{3+} in monoclinic Y_2O_3 was lower than for cubic Y_2O_3: samples with $\geq 0.7\%$ Eu^{3+} were found to be composed of two phases, monoclinic Y_2O_3 and Eu_2O_3 [12]. Not all nanocrystalline Y_2O_3 powders are monoclinic. For example, in combustion synthesized $(Y_{1-x}Eu_x)_2O_3$ powders 14-26 nm in size, the monoclinic phase was not found [13]. It

appears that stabilization of the monoclinic phase is dependent on the processing technique, and is more likely to form at lower synthesis temperatures.

Thin-film $(Y_{1-x}Eu_x)_2O_3$ has been deposited by low pressure metallorganic chemical vapor deposition (MOCVD) [14,15], spray pyrolysis [16] and pulsed laser ablation [17-19]. Independent of the deposition technique, the as-synthesized films were found to be weakly luminescent and required post-deposition annealing to increase the emission intensity. The increase in luminescence has been be related to the crystallite size [20], similar to the effect found in powder samples. Films containing smaller crystallites have more grain boundaries, which are thought to be non-luminescent or even luminescence quenching regions [7]. It has been difficult to de-couple the thermal annealing effects, such as diffusion and lattice parameter changes, with the increase in grain size. In Y_2O_3:Eu^{3+}, the C_2 sites (lower symmetry) have stronger transitions than the C_{3i} sites (higher symmetry) [6]. It is possible that an entirely random distribution of Eu^{3+} on the Y^{3+} sites is not present in as-deposited thin-films, thereby altering the fluorescence spectrum. This could be especially true for high concentrations of Eu^{3+}, in which Eu^{3+}-Eu^{3+} interactions could also modify the luminescent spectrum.

The purpose of this study was to identify and correlate the microstructural and luminescence properties of $(Y_{1-x}Eu_x)_2O_3$ thin-films deposited by MOCVD as a function of deposition time and temperature. The influence of deposition parameters on the crystallite size and microstructural morphology has not been previously studied in this system. In addition, this research sought to quantify and separate crystallite size effects with other thermal effects on the resulting luminescent properties.

Experimental Techniques

A schematic diagram of the stainless steel MOCVD system is depicted in Figure 3. The chamber is a cold-wall vertical reactor. The organometallic precursor is delivered to the reactor through a nozel with a shower head. The shower head was located 10 cm above the hot stage.. Sapphire substrates with the (001) face exposed, 2.54 cm in diameter and (111) Si pieces were placed on the hot stage, Stainless steel bubblers contained yttrium and europium tris(2,2,6,6,-tetramethyl-3,5-heptanedionates) precursors. The bubblers were heated to 146°C to sublime the organometallic species. Argon carrier gas passed through the heated bubblers to transport the vapor to the reaction chamber. The shower head , 3 cm in diameter, contained an array of 3 mm circular holes. Oxygen gas was used as the oxidant during the growth process. Oxygen flowed into the chamber through two inlets positioned at ±60° to the substrates. During deposition the substrate temperature was maintained at temperatures between 500 and 700°C as monitored by a thermocouple. Mass flow controlers regulated the argon and oxygen flows. The total pressure inside the chamber was maintained with down stream control. Table I shows the deposition parameters.

After the deposition, the samples were allowed to cool to room temperature inside the chamber. Rutherford backscattering (RBS) was used to determine the europium concentration in the films. A chemical binding energy analysis to examine the sample purity was also performed at the surface using X-ray photoelectron spectroscopy (XPS) operated with an Al Kα (1486.6 eV) X-ray source with a resolution of 1 at %. The crystallinity of the films were analyzed by X-ray diffraction (XRD) and observed by scanning electron microscopy (SEM). The crystallite size was measured by X-ray line broadening using Warren-Averbach analysis [21]. Small scratches were made on the films with a diamond stylus and the film thickness measured with a surface profilometer. Photoluminescemce measurements were made with a CCD detector with an UV Hg excitation

source. A spot 2 mm in diameter was incident on the film and the emission spectra were collected in reflection mode with a 200 μm fiber optic cable. Post-deposition processing consisted of annealing one sample deposited on sapphire at 600°C for 8 hours at 850°C for 24 and 108 hours.

Results and Discussion

Figure 4 shows the XPS spectra for films grown at 700°C for 4 hours with two different europium β-diketonate carrier gas flow rates (10 and 20 sccm). The films show no detectable carbon peak present (270 eV). This indicates that the β-diketonates are excellent precursors for depositing high purity materials with a high degree of compositional control. The ease of stoichiometric control is attractive for compositions which require tightly controlled dopant concentrations This processing flexibility is absent for deposition methods using single composition targets, such as physical vapor deposition techniques.

All films were luminescent in the as-deposited state, indicating the films were crystalline. The films were smooth and appeared continuous to the eye. Table II lists the thickness and europium concentration for a series of films deposited for 1, 2, 4 and 8 hours at 600°C. The growth rate was found to be 0.17 μm/hour. However, the europium concentration (x) decreased as the deposition time increased, which was not expected. West and Beeson have determined that x can be expressed by [14]:

$$x = \frac{C_{Eu}\exp\left[\frac{-\Delta H_{Eu}}{RT_{Eu}}\right]}{C_{Eu}\exp\left[\frac{-\Delta H_{Eu}}{RT_{Eu}}\right] + C_{Y}\exp\left[\frac{-\Delta H_{Y}}{RT_{Y}}\right]} \quad (1)$$

where C_{Eu} and C_Y are constants, ΔH_{Eu} and ΔH_Y are the enthalpies of vaporization, R is the gas constant the T_{Eu} and T_Y are the reservoir temperatures of the precursors. It was found experimentally that $\Delta H_{Eu} = \Delta H_Y$ and that at 140°C, $C_Y = 19C_{Eu}$. With the reservoir temperatures held at 147°C, it is expected that x=0.05. A possible explanation for the high europium content found in all of the films coupled with the decrease in europium concentration with increasing deposition time could be related to the nucleation kinetics. Rutherford back scatteringdata also indicated that the europium concentration through the film thickness was not constant; a higher concentration existed near the substrate/film interface. It appears under these deposition conditions, nucleation of Y_2O_3 may not be as rapid as Eu_2O_3.

XRD studies revealed a series of compositional and structural changes in the films deposited at different deposition temperatures on (100) sapphire substrates. Depositions for 6 hr at 500°C or 2 hours at 600°C were composed of cubic Y_2O_3, oriented in the [100] or [110] direction perpendicular to the substrate, as evidenced by the strong (400) and (440) peaks, as shown in Figure 5. This is supported by previous work that has shown MOCVD films grown on (001) sapphire substrates were oriented in the [100] but were randomly oriented when deposited on $In_2O_3:Sn^{4+}$ coated glass substrates or polycrystalline Al_2O_3 substrates [17]. In other work on MOCVD films of this composition deposited on polycrystalline Al_2O_3 at 525°C, polycrystalline cubic $(Y_{1-x}Eu_x)_2O_3$ was found [14].

A four hour deposition at 600°C showed peaks for cubic Y_2O_3. However, additional peaks are present that can be indexed to monoclinic Y_2O_3, as shown in Figure 5. Monoclinic Y_2O_3 was also detected on films deposited on (111) Si. This is the first report of the observation of monoclinic $(Y_{1-x}Eu_x)_2O_3$ in thin films. The cubic Y_2O_3 pattern still reveals a strongly oriented growth in the [100]direction. This orentation becomes more defined than the 500°C depositions. After a four hr deposition at 700°C, the XRD pattern has narrower and more intense peaks with the most intense being the (222), indicating the films are textured in the [111]. Monoclinic Y_2O_3 is still detected in the pattern, as shown in Figure 5, although the fraction is smaller compared to the 600°C sample. The XRD data is summarized in Table II. It appears that there is a minimum substrate temperature at which monoclinic Y_2O_3 forms, and as the temperature increases, the volume fraction of monoclinic decreases as the amount of cubic increases.

These orientation results are in contrast to other work on pulsed laser deposited films on (100) Si and (111) diamond. The films were found to grow in a [111] direction at deposition temperatures $\leq$ 500°C while at higher deposition temperatures ($\geq$ 700°C) there was a preferential [100] growth direction [18,19]. Reports indicate that the (111) surface is the low energy surface in Y_2O_3, thus growth of these surfaces would be preferred [19]. This was observed for the 700°C deposits. However, the initial orientation is along the [100], suggesting that the interface between the (001) sapphire and (100) Y_2O_3 should be the low energy configuration.

SEM micrographs reveal different microstructural features in the films grown at different temperatures on Si. At 500°C, the films are cracked, as shown in Figure 6, apparently due to thermal expansion mismatch. The thermal stress in a thin film is given by [22]:

$$\sigma_f(T) = \frac{(\alpha_s - \alpha_f)(T - T_o)E_f}{1 - \nu_f} \qquad (6)$$

where the subscripts f and s refer to the film and substrate, respectively. In equation (6), the film stress, σ_f, depends on the thermal expansion coefficient, α, , the measurement temperature ,T, the deposition temperature ,T_o, the elastic modulus, E, and Poisson's ratio ,ν a. The thermal expansion coefficients for silicon and Y_2O_3 are 4 and 8.1 x10^{-6}/°C, respectively and the modulus and Poisson's ratio for Y_2O_3 are 151.7 GPa and 0.30, respectively [23]. The films would be in residual tension and the film stress is an order of magnitude larger than the flexural strength of Y_2O_3 (123 MPa) [23]. The films deposited on sapphire do not show thermal cracking, as shown in Figure 7, since the thermal expansion coefficient of (001) sapphire is 9 x 10^{-6}/°C. The film appearance is very similar to what was reported for MOCVD $(Y_{1-x}Eu_x)_2O_3$ films deposited at 525°C [14].

Figure 8 shows a film deposited at 600°C for the two hours. The film is 0.40 μmthick. Cracking of the films is evident but the crystallites can be resolved with a size of ~150 nm. The film is similar to microstructures found on deposits on Si at 600°C and diamond by pulsed laser ablation [18,19]. Increasing the deposition time to four hour yields an entirely different microstructure, as shown in Figure 9. The film thickness has increased to 0.73 μm and the microstructure consists of an unusual platelet-type growth. This was not previously observed in films of this composition. Despite the thermal mismatch, the films are not cracked, which may be due to the discontinuity of the grains in the microstructure. Increasing the deposition temperature to 700°C for 4 hours yields a similar but coarser microstructure as for the 600°C deposition, as shown in Figure 10. However these films are strongly oriented in the [111]. The microstructural development appears to be the initial nucleation of cubic Y_2O_3 oriented in the [100] or [110], due to interfacial energy constraints

between sapphire and Y_2O_3. Higher deposition temperatures promotes growth of the low energy (111) surface of cubic Y_2O_3 along with the nucleation of monoclinic Y_2O_3. It is possible that the presence of monoclinic Y_2O_3 affects the growth and morphology of the cubic Y_2O_3. The platelet-type growth is also observed on sapphire substrates, indicating that stress relief alone does not promote this type of growth.

Photoluminescent measurements taken on films grown on sapphire reveal that increasing the substrate temperature increases the intensity of the emission spectrum, as shown in Figure 11. $Y_2O_3:Eu^{3+}$ is cubic and orientation effects are not expected to influence the PL spectra. The features for all samples are broad (as compared to Figure 2) indicating a large degree of disorder around the Eu^{3+} ion. There is a larger increase in the emission intensity on increasing the substrate temperature from 500 to 600°C as compared to increasing the temperature from 600 to 700°C. Since the strong 611 nm features is a very good indicator of the presence of cubic $Y_2O_3:Eu^{3+}$, this phase is present in all of the films. The large feature at 628 nm has been attributed to monoclinic $Y_2O_3:Eu^{3+}$ [8,12]. Although monoclinic $Y_2O_3:Eu^{3+}$ was not detected by XRD in the 500°C deposits, a small amount of this phase must be present in these films since spectroscopic techniques are more sensitive in detecting small amounts of materials than XRD. Increasing the deposition temperature increases the intensity of the 611 nm features relative to the 628 nm feature, indicating that the volume fraction of cubic Y_2O_3 is increasing. The amounts of monoclinic and cubic cannot be determined from these measurements. The emission intensity increase can be attributed to both grain growth (minimizing grain boundary area) and a reduction of disorder around the Eu^{3+} in the lattice.

Because of the presence of the 611 nm feature in the samples, it is not unreasonable to account for the feature center around 628 nm to be an effect of a high Eu^{3+} concentration, especially for the low temperature depositions. The transitions shown in Figure 1 can be used in solids where a low concentration of Eu^{3+} is present. The influence of Eu^{3+}-Eu^{3+} interaction and subsequent affect on the luminescent spectrum is not known.

To analyze the influence of crystallite size on luminescent properties, a film deposited at 600°C for 8 hours on sapphire was post-annealed at 850°C for 24 or 108 hours to promote crystallite growth. Figure 12 shows an increase of the XRD peak intensity is induced with the longer annealing treatments. Sharper peaks are also observed along with a slight shift in peak location. The sharpening of the peaks indicates an increase in crystallite size and the shift in the peak location indicates a decrease in the lattice parameter. Photoluminescent measurements taken on the same films as shown in Figure 12 are presented in Figure 13. The PL intensity increases along with an increase in crystallite size. Table III summarizes the structural and luminescent data taken on the as-deposited and annealed samples. The area under the PL spectra was integrated between 550-650 nm to obtain the integrated intensity. Comparing the as-deposited sample with the 108 hour annealed sample, the crystallite size increased by 26%, which is closely correlated with the increase in PL integrated intensity (20%). The change in lattice parameter was only 0.12%, indicating that this had less of an influence on the PL emission behavior than the change in crystallite size. Thermal effects (diffusion, sublimation of volatile species, grain growth) are known to improve luminescent emission intensity in powders [24] and films [14,17]. However, these results show that the increased crystallite size, whether induced by an increase in temperature or an increase in annealing time, is the dominant mechanism for improved PL emission intensity. This can be attributed to a reduction in the grain boundary area, a region with a high density of defects that could quench luminescence emission.

Conclusions

Thin-films of $(Y_{1-x}Eu_x)_2O_3$ were deposited by low-pressure metallorganic vapor deposition with Y- and Eu-tris(2,2,6,6,-tetramethyl-3,5-heptanedionates) precursors on (001) sapphire and (111) Si substrates. The as-deposited films were crystalline and luminescent and carbon contamination was not detected. The growth rate was found to be 0.17 μm/hr at 600°C with the yittrium and europium reservoirs at 147°C and carrier gas flow rates of 100 and 10 sccm, respectively. The films deposited at 500°C were flat and were composed of nanocrystalline regions which showed thermal cracking on Si substrates but not on sapphire substrates. These films were composed of cubic Y_2O_3, grown in a textured [100] or [110] orientation to the substrate surface. Films deposited at 600°C developed from the flat, nanocrystalline morphology (2 hours) into a plate-like growth morphology oriented in the [111] with increasing deposition time (4 hours). Monoclinic Y_2O_3:Eu^{3+} was observed for deposition temperatures ≥ 600°C on both (111) Si and (001) sapphire substrates, which also correlated with the photoluminescent emission spectra. An increase of the deposition temperature increased the photoluminescent intensity which was attributed to a reduction in grain boundary area and a decrease in ionic disorder around the Eu^{3+}. Post-deposition annealing at a fixed temperature increased the crystallite size and decreased the lattice parameter.The former was more effective in increasing the PL intensity than the latter.

Acknowledgments

We would like to thank Norn Elliot of LANL for the SEM micrographs. This work was conducted under the auspices of the US Department of Energy, supported (in part) by funds provided by the University of California for the conduct of discretionary research by Los Alamos National Laboratory under project CULAR and the Visiting Scholar Program and through the Phosphor Technology Center of Excellence by DARPA Grant No. MDA972-93-1-0030.

References

1. K. A. Franz, W. G. Kehr, A. Siggel, J. Wieczoreck, in Ullmann's Encyclopedia of Industrial Chemistry, eds. B. Elvers, S. Hawkins, and G. Schulz, **A15**, VCH Publishers, Weinheim, Germany 1985.
2. K.A. Wickersheim and R.A. Lefever, "Luminescent Behavior of the Rare Earths in Yttrium Oxide and Related Hosts," *J. Electrochem. Soc.*, **111** [1] 47-51 (1964).
3. N.C. Chang and J.B. Gruber, "Spectra and Energy Levels of Eu^{3+} in Y_2O_3," *J. Chem. Phys.*, **41** [10] 3227-3234 (1964).
4. M.J. Sellars, R.S. Meltzer, P.T.H. Fisk and N.B. Manson, "Time-Resolved Ultranarrow Optical Hole Burning of a Crystalline Solid: Y_2O_3:Eu^{3+}," *J. Opt. Soc. Am. B*, **11**[8] 1468-1473 (1994).
5. N.C. Chang, "Fluorescence and Stimulated Emission from Trivalent Europium in Yttrium Oxide," *J. Appl. Phys.*, **34** [12] 3500-3504 (1963).
6. J. Heber, K.H. Hellwege, U. Köbler and H. Murmann, "Energy Levels and Interaction between Eu^{3+}-ions at Lattice Sites of Symmetry C_2 and Symmetry C_{3i} in Y_2O_3," *Z. Physik*, **237** 189-204 (1970).
7. L.E. Shea, J. McKittrick and M.L.F. Phillips, "Predicting and Modeling the Low-Voltage Cathodoluminescent Efficiency of Oxide Phosphors," *J. Electrochem. Soc.*, accepted.
8. H. Eilers and B.M. Tissue, "Laser Spectroscopy of Nanocrystalline Eu_2O_3 and Eu^{3+}:Y_2O_3," *Chem. Phys. Lett.*, **251** 74-78 (1996).
9. M. Ya. Grytsiv, V.D. Bondar and S.I. Chykhrii, "Structure of Yttria Thin Films Prepared by Reactive RF Diode Sputtering," *Inorg. Mat.*, **32** [11] 1202-1204 (1996).
10. H.R. Hoekstra and K.A. Gingerich, "High-Pressure B-Type Polymorphs of Some Rare-Earth Sesquioxides," *Science*, **146** [3647] 1163-64 (1964).
11. G. Skandan, C.M. Foster, H. Frase, M.N. Ali, J.C. Parker and H. Hahn, "Phase Characterization and Stabilization Due to Grain Size Effects of Nanostructured Y_2O_3," *Nanostruc. Mat.*, **1** 313-322 (1992).
12. B. Bihari, H. Eilers, B.M. Tissue, "Spectra and Dynamics of Monoclinic Eu_2O_3 and Eu^{3+}:Y_2O_3 Nanocrystals," *J. Lumin.*, **75** 1-10 (1997).
13. M. Kottaisamy, D. Jeyakumar, R. Jagannathan and M. Mohan Rao, "Yttrium Oxide:Eu^{3+} Red Phosphor by Self-Propagating High Temperature Synthesis," *Mater. Res. Bull.*, **31** [8] 1013-1020 (1996).
14. G.A. West and K.W. Beeson, "Low-Pressure Metalorganic Chemical Vapor Deposition of Photoluminescent Eu-doped Y_2O_3 Films," *J. Mater. Res.*, **5** [7] 1573-1580 (1990).
15. J.P Dismukes, J. Kane, B. Binggeli and H.P. Schweizer, "Chemical Vapor Deposition of Cathodoluminescent Phosphor Layers," in Chemical Vapor Deposition: Fourth International Conference, eds. G.F. Wakefield and J.M. Blocher, The Electrochemical Society, Princeton, NJ, 1973.
16. H.P. Maruska, T. Parodos, N.M. Kalkhouraud and W.D. Halverson, "Challenges for Flat Panel Display Phosphors," *Mat. Res. Soc. Symp. Proc.*, **345** 269-280 (1994).
17. G. A. Hirata, J. McKittrick, M. Avalos-Borja, J. M. Sisqueiros and D. Devlin, "Physical Properties of Y_2O_3:Eu Luminescent Films Grown by MOCVD and Laser Ablation," *Appl. Surf. Sci.*, **113/114** 509-514 (1997).
18. K.G. Cho, D. Kumar, D.G. Lee, S.L. Jones, P.H. Holloway and R.K. Singh, "Improved Luminescence Properties of Pulsed Laser Deposited Eu:Y_2O_3 Thin Films on Diamond Coated Silicon Substrates," *Appl. Phys. Lett.*, **71** [23] 3335-3337 (1997).

19. S.L. Jones, D. Kumar, R.K. Singh and P.H. Holloway, "Luminescence of Pulsed Laser Deposited Eu Doped Yttrium Oxide Films," *Appl. Phys. Lett.*, **71** [3] 404-406 (1997).
20. G.A. Hirata, J. McKittrick, J. Yi, S.G. Pattillo, K.V. Salazar and M. Trkula, "Microstructural and Photoluminescence Studies on Europium Doped Yttrium Oxide Films Synthesized by Metallorganic Vapor Deposition," *Mat. Res. Soc. Symp. Proc.*, accepted.
21. D. Balzar, "Profile Fitting of X-ray Diffraction Lines and Fourier Analysis of Broadening," *J. Appl. Cryst.*, **25**, 559-570 (1992).
22. M. Ohring, The Materials Science of Thin Films, Academic Press, Inc., San Diego, CA, 1992.
23. Engineering Property Data on Selected Ceramics, Vol. I, Single Oxides, MCIC Report-HB-07, Metals and Ceramics Information Center, Battelle, Columbus, Ohio, 1981.
24. L.E. Shea, J. McKittrick, O.A. Lopez, E. Sluzky, "Synthesis of Red-Emitting, Small Particle Size Luminescent Oxides Using an Optimized Combustion Process," *J. Am. Ceram. Soc.*, **79** [12] 3257-65 (1996).
25. L. Ozawa, Cathodoluminescence, Theory and Application, VCH Publishers, Weinheim, Germany, 1990.

List of Tables

List of Figures

substrate	sapphire or Si
substrate temperature	500-700°C
carrier gas	argon
metallorganic precursors	Y- or Eu-tris (2,2,6,6-tetramethyl-3,5-heptanedionate)
Y carrier gas flow rate	100 sccm
Eu carrier gas flow rate	10 sccm
Y reservoir temperature	146°C
Eu reservoir temperature	146°C
oxygen gas flow rate	100 sccm
chamber pressure	5 Torr
deposition time	1 - 8 hours

Table I MOCVD deposition parameters.

substrate temperature (°C)	Eu flow (sccm)	time (hours)	thickness (μm)	europium concentration	phases present (on Si substrates)
500	10	6	1.38		c-Y_2O_3 [100] and [110]
600	10	1	0.03-0.10	0.31	*
600	10	2	0.40	0.29	c-Y_2O_3 [100] and [110]
600	10	4	0.73	0.18	c+m-Y_2O_3 [100]
700	10	4	1.51		c+m-Y_2O_3 [111]

* signal too weak

Table II. Film thickness, x in $(Y_{1-x}Eu_x)_2O_3$ and phases present.

condition	lattice parameter (nm)	crystallite size (nm)	normalized PL integrated intensity
as-synthesized	1.0632	17	1.0
850°C, 24 hours	1.0624	20	1.1
850°C, 108 hours	1.0619	23	1.2

Table III Summary of data taken on $Y_2O_3:Eu^{3+}$ films on sapphire deposited for eight hours at 600°C and then heat treated to 850°C for 24 or 108 hours.

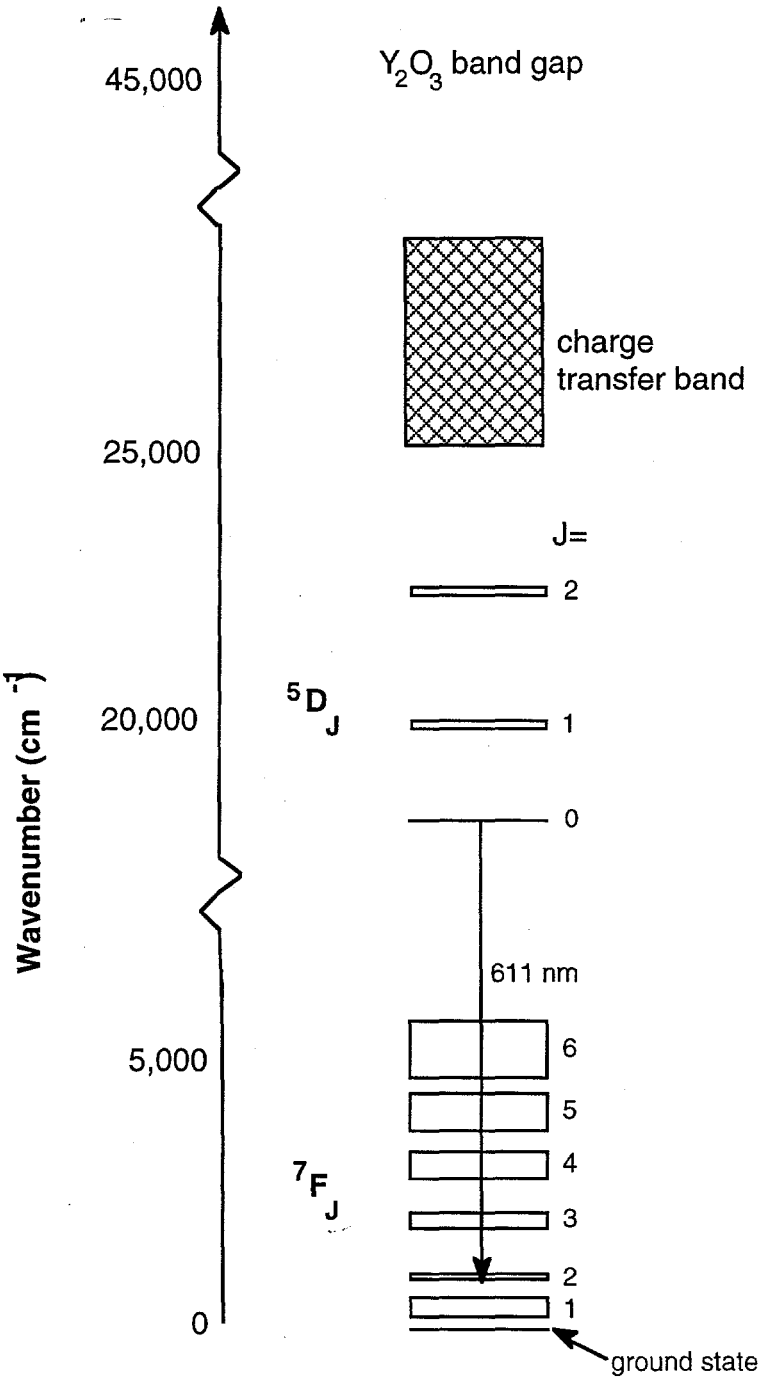

Figure 1 Partial energy level diagram for Eu^{3+} in Y_2O_3. The strong transition causing the 611 nm featurein the fluorescence spectra is shown. The charge transfer is the lowest level absorption band in this system with the band gap absorption occurring at a higher energy level. Adapted from [5].

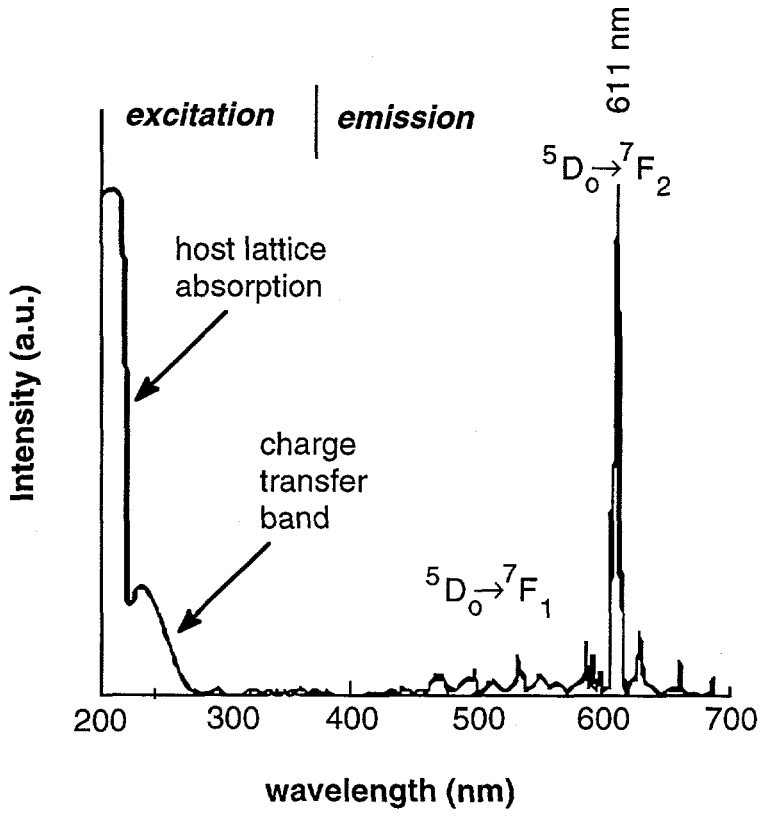

Figure 2 Typical fluorescence spectrum for $(Y_{1-x}Eu_x)_2O_3$ powders. Adapted from [26].

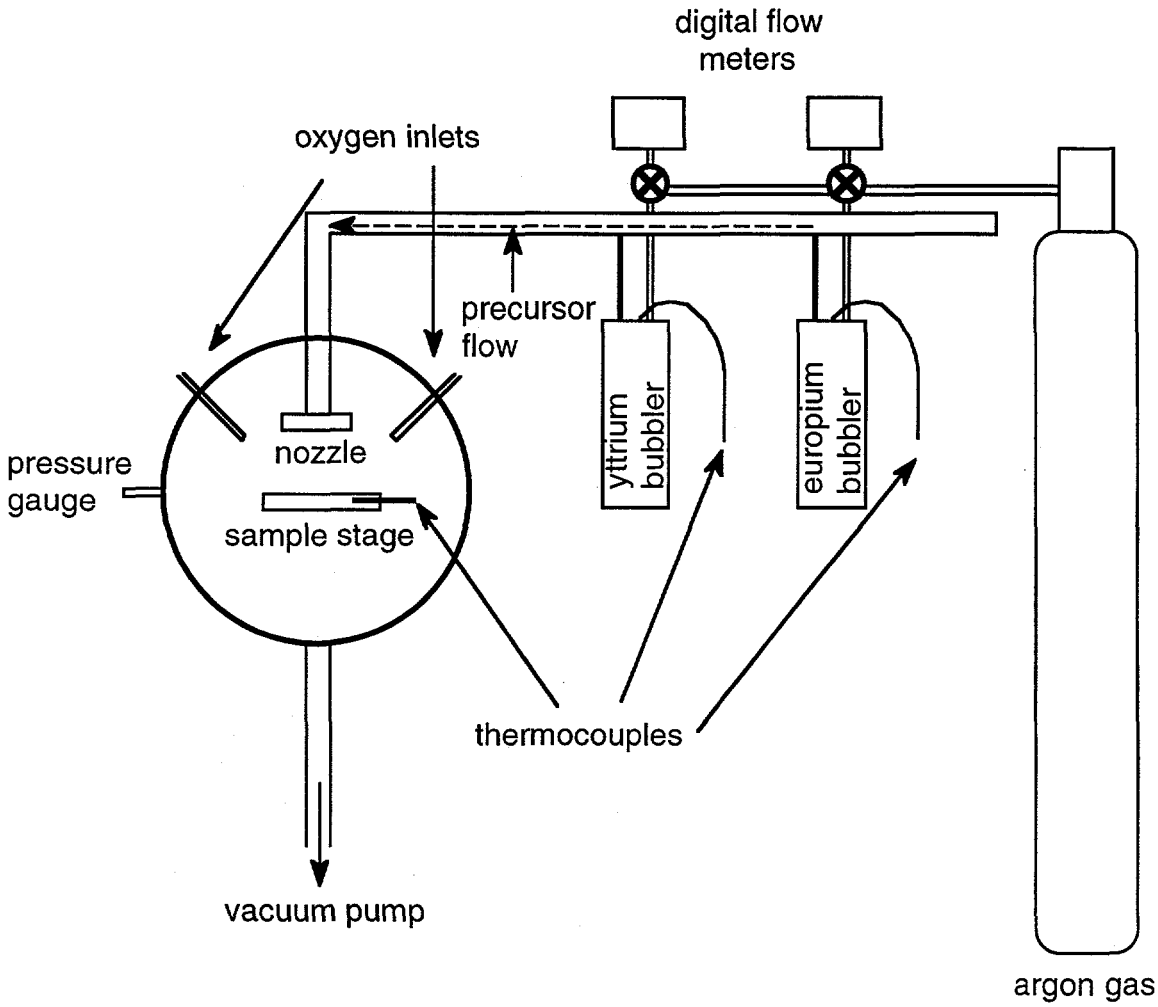

Figure 3 Schematic diagram of the MOCVD chamber.

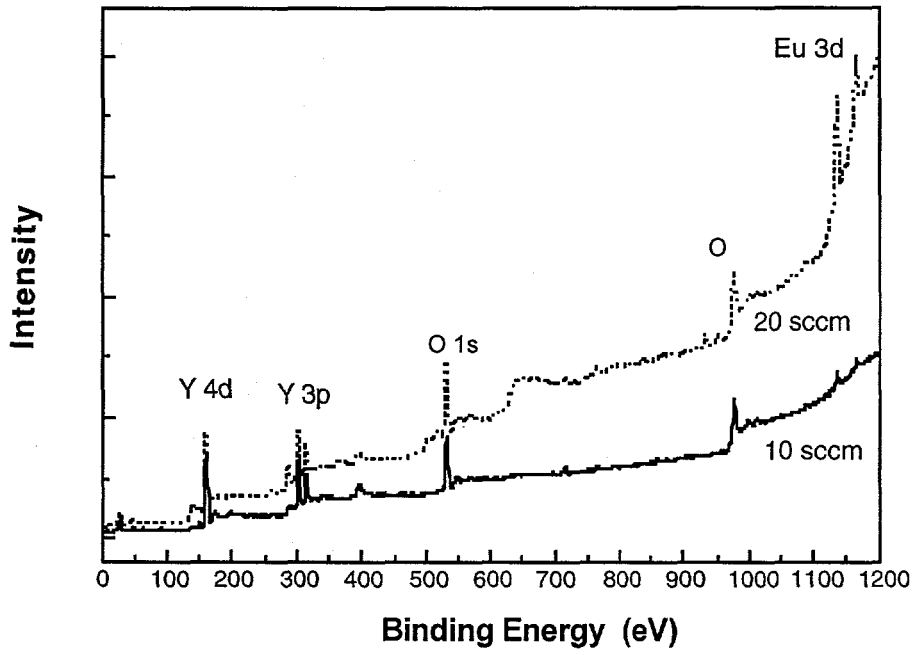

Figure 4 XPS spectra for films grown with a Eu β-diketonate flow rate of (a) 10 sccm and (b) 20 sccm.

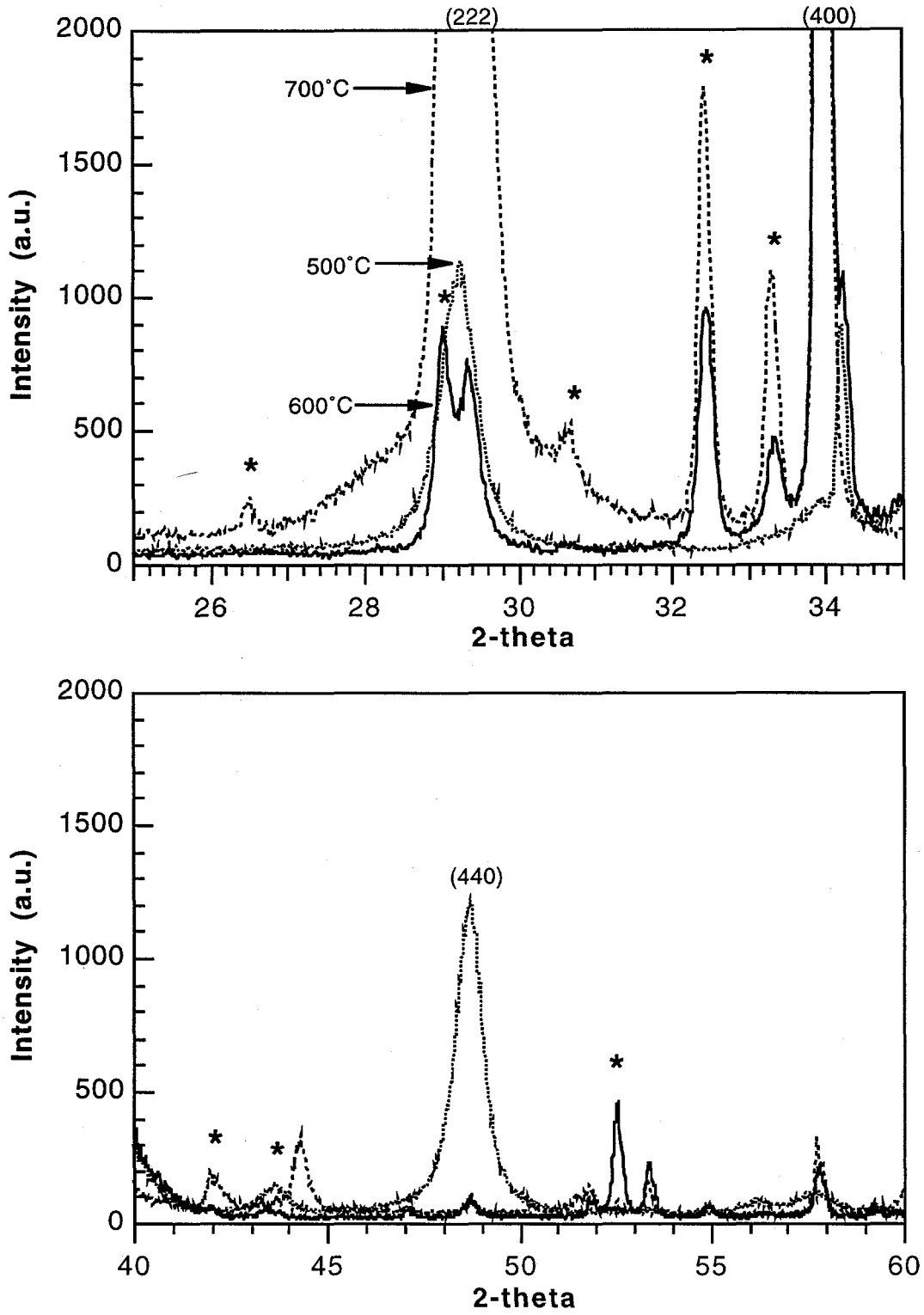

Figure 5 X-ray diffraction pattern of films deposited at 500 (six hours), 600 and 700°C (four hours). * are monoclinic Y_2O_3, JCPDS #44-399. Cu Kα radiation, $\lambda = 0.154$ nm. The $2\theta = 35$-40 region was intentionally omitted due to the strong sapphire peak. The strong peaks for cubic Y_2O_3 are labeled (JCPDS #41-1105).

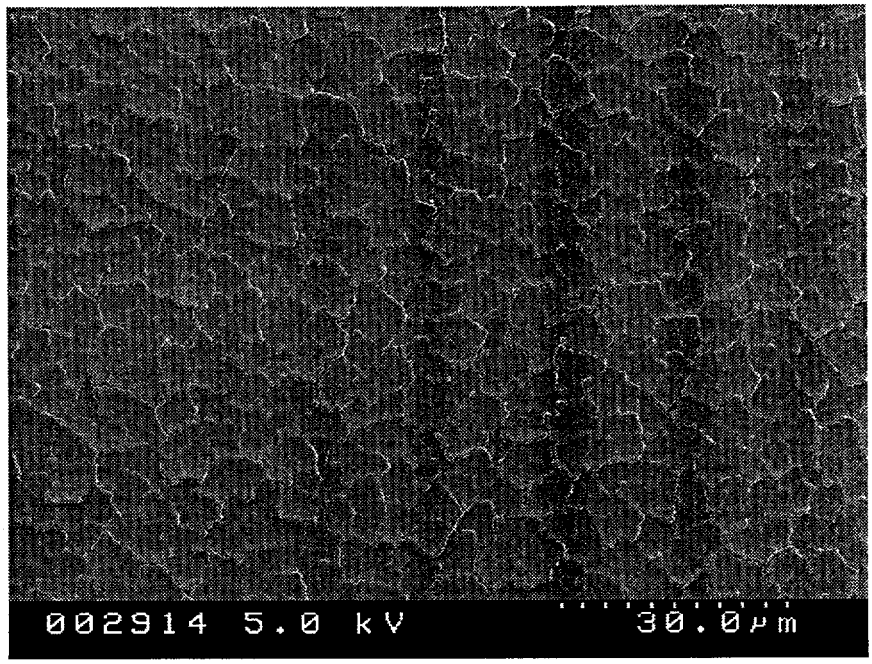

(a)

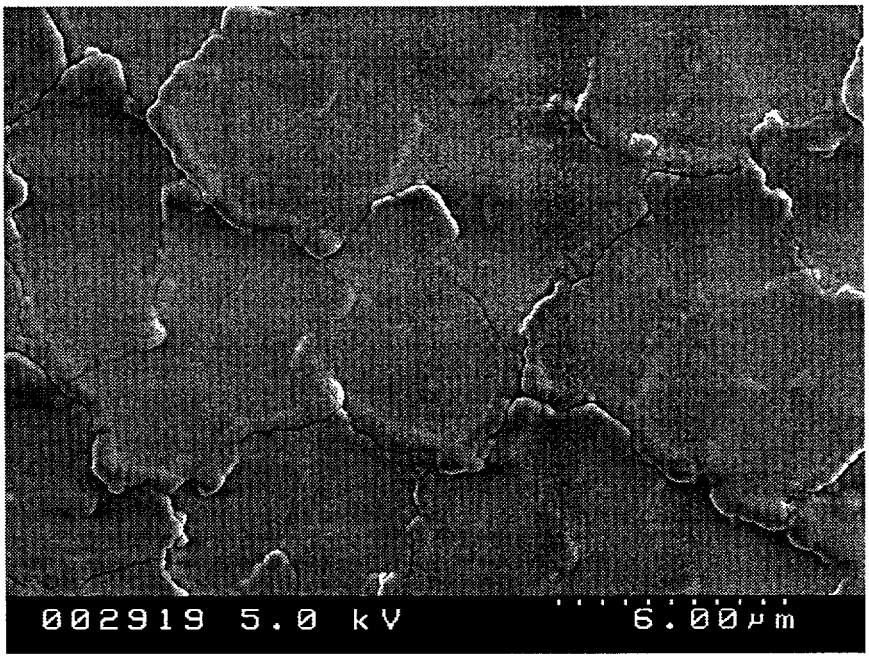

(b)

Figure 6 SEM micrographs of the films deposited at 500°C for six hours, (a) 1000X, (b) 5000X and (c) 10,000X.

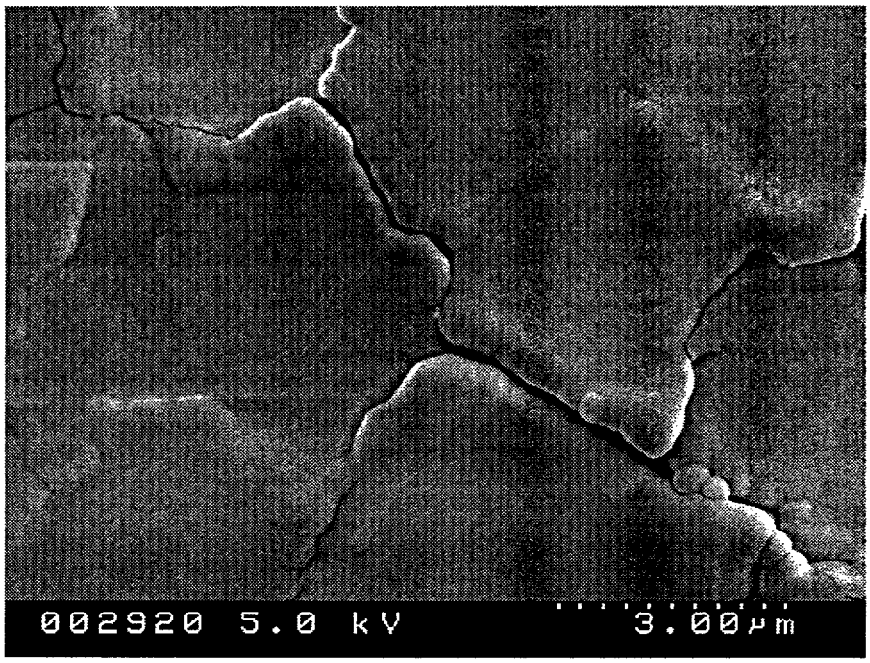

(c)

Figure 6 SEM micrographs of the films deposited at 500°C for six hours, (a) 1000X, (b) 5000X and (c) 10,000X.

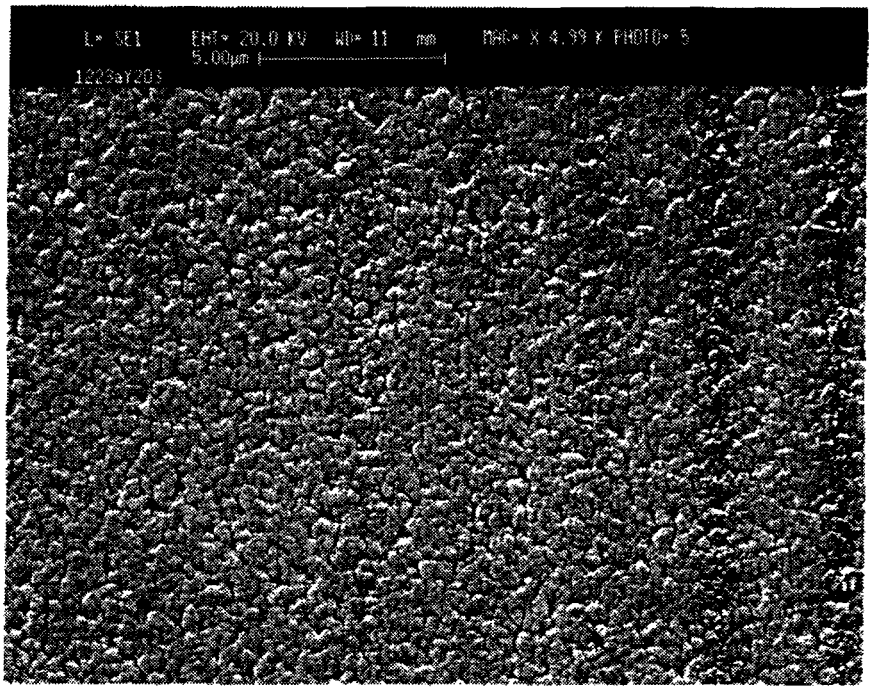

(a)

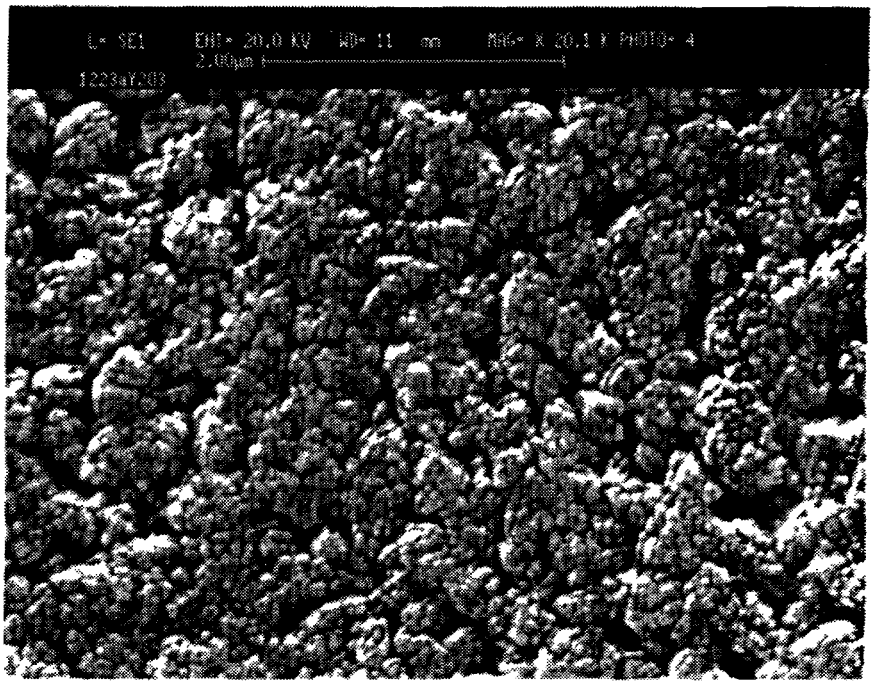

(b)

Figure 7 SEM micrographs of films deposited for six hours at 500°C on sapphire (a) 4000X and (b) 20,000X.

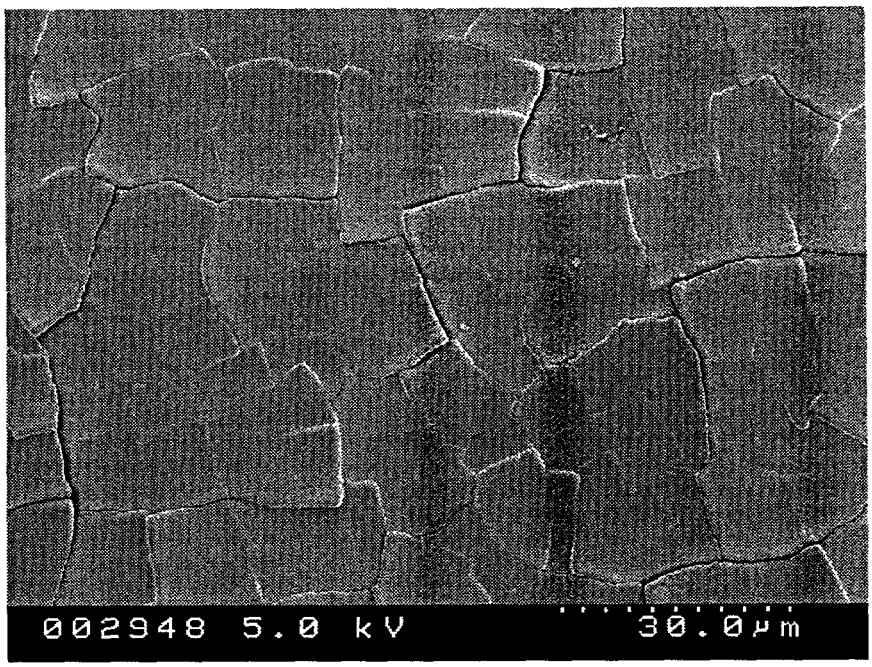

(a)

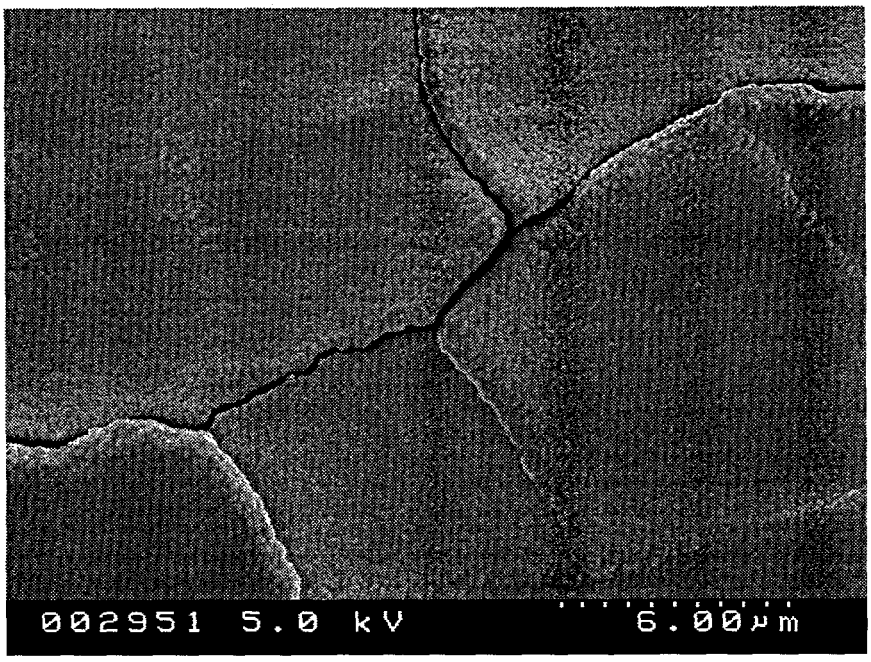

(b)

Figure 8 SEM micrographs of the films deposited at 600°C for two hours, (a) 1000X, (b) 5000X and (c) 10,000X.

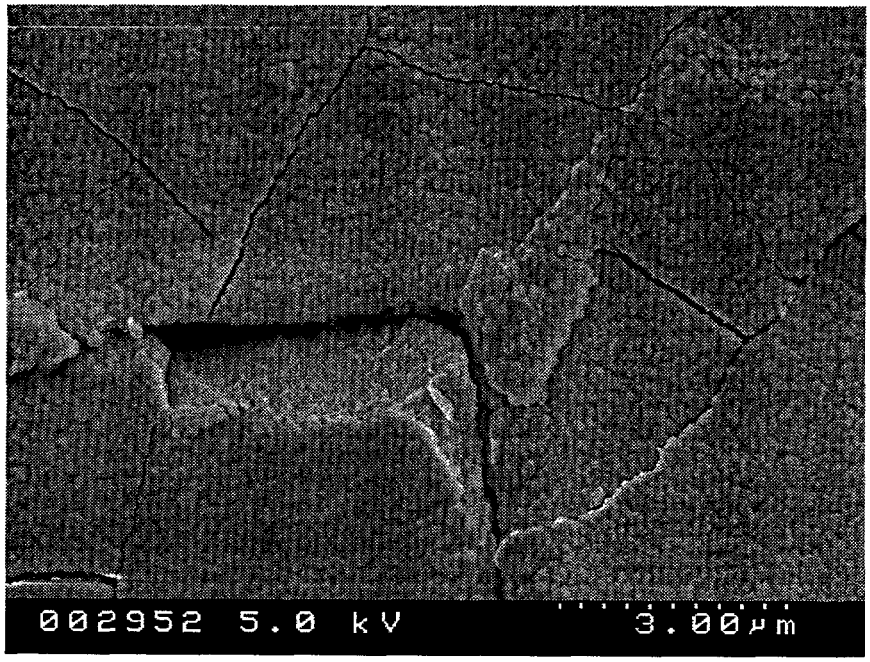

(c)

Figure 8 SEM micrographs of the films deposited at 600°C for two hours, (a) 1000X, (b) 5000X and (c) 10,000X.

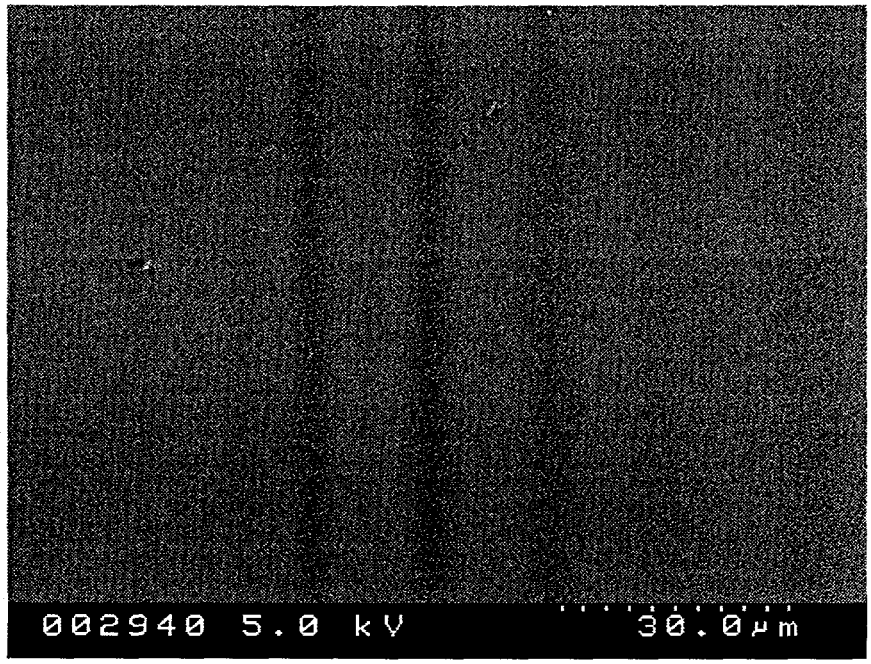

(a)

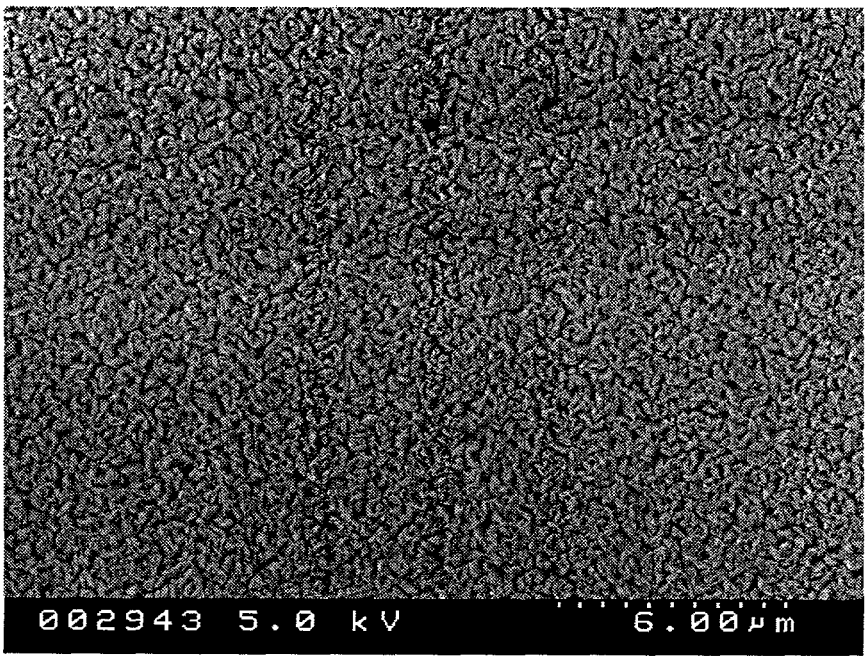

(b)

Figure 9 SEM micrographs of the films deposited at 600°C for four hours, (a) 1000X, (b) 5000X and (c) 10,000X.

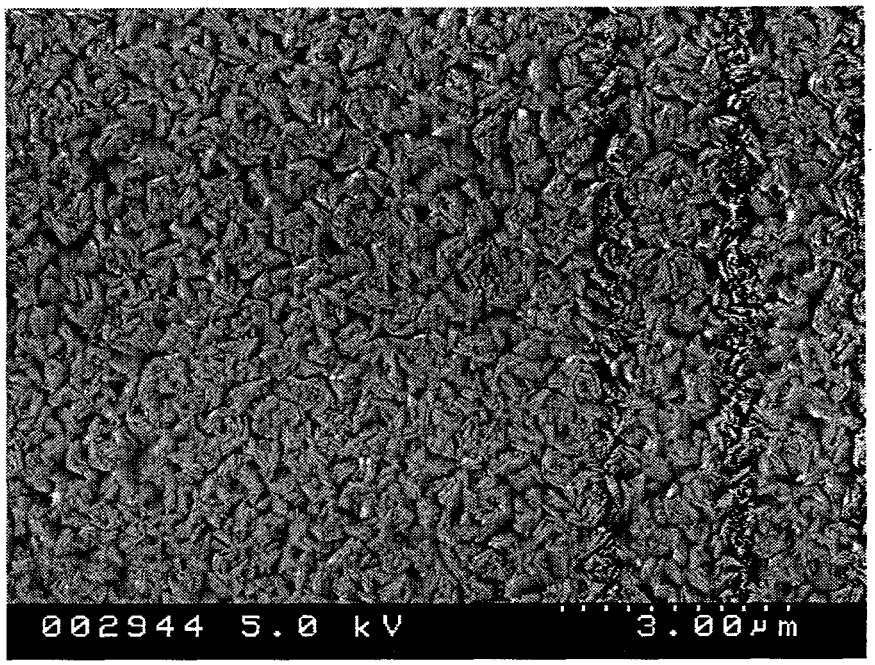

(c)

Figure 9 SEM micrographs of the films deposited at 600°C for four hours, (a) 1000X, (b) 5000X and (c) 10,000X.

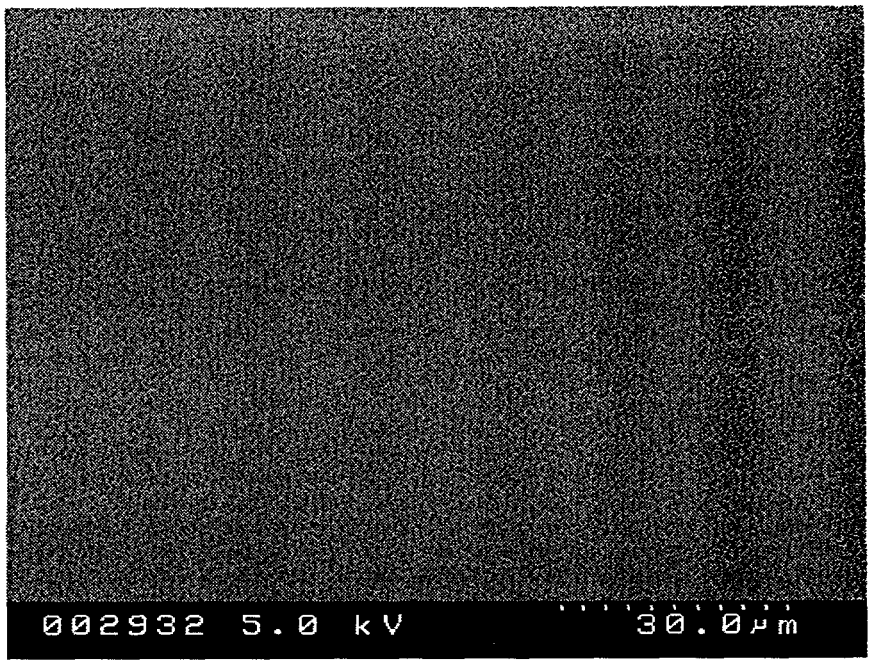

(a)

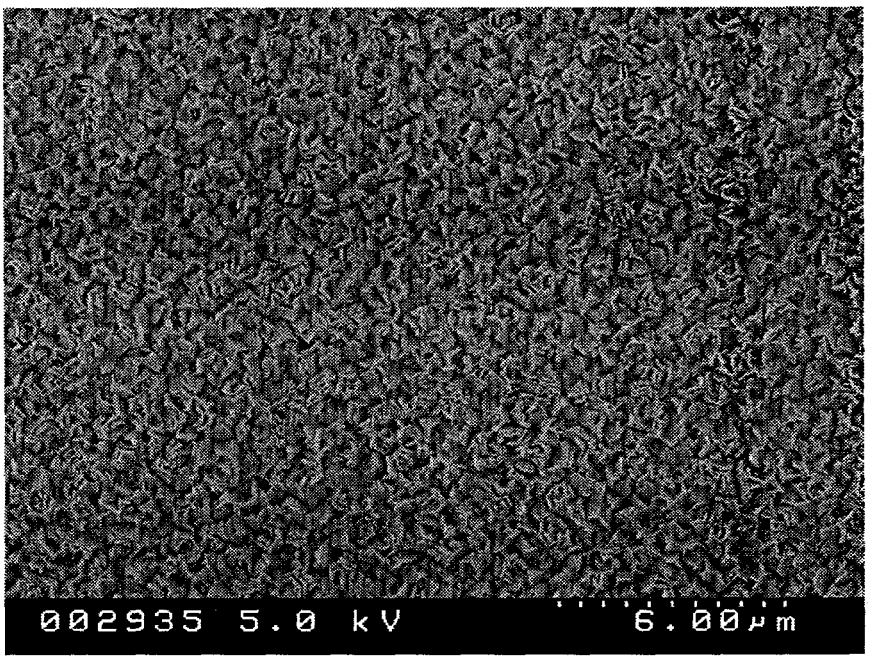

(b)

Figure 10 SEM micrographs of the films deposited at 700°C for four hours, (a) 1000X, (b) 5000X and (c) 10,000X.

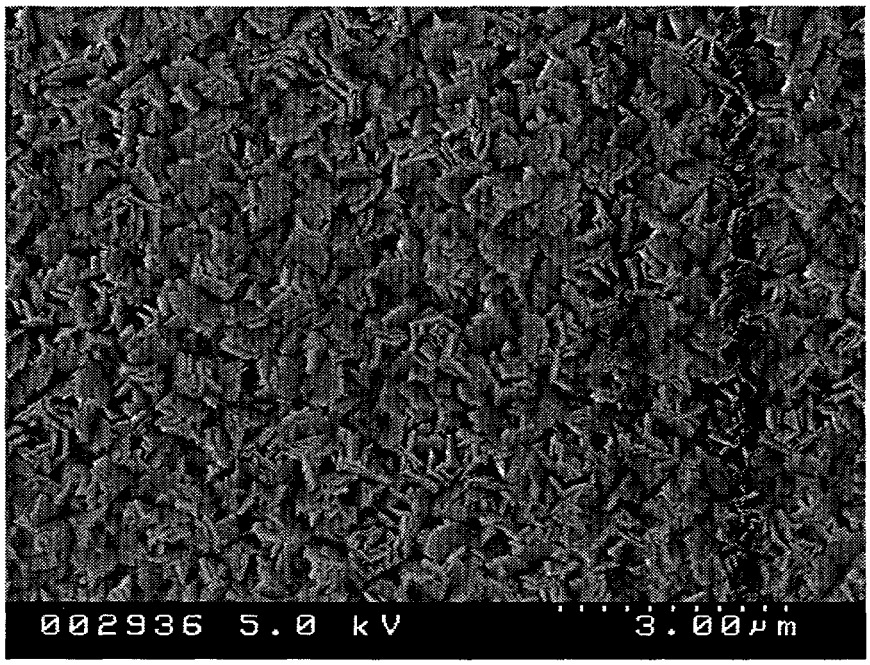

(c)

Figure 10 SEM micrographs of the films deposited at 700°C for four hours, (a) 1000X, (b) 5000X and (c) 10,000X.

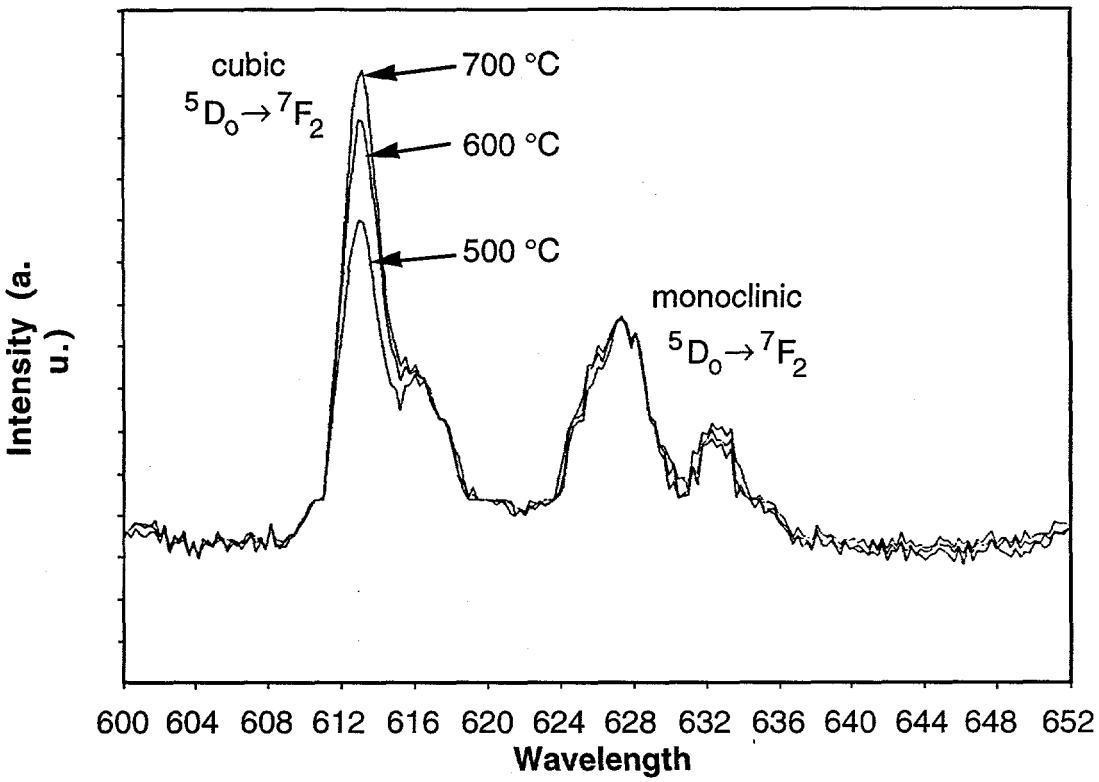

Figure 11 Photoluminescent emission spectra of film deposited at 500 (six hours), 600 (four hours) and 700°C (four hours).

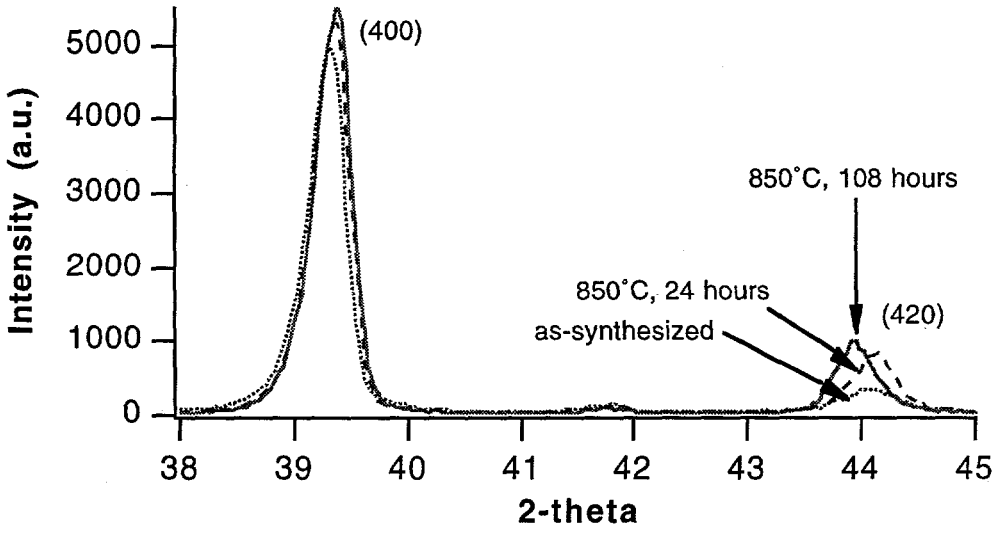

Figure 12 XRD spectra for the film grown at 600°C for eight hours and post-annealed at 850°C for 24 and 108 hours. The (400) and (420) reflections are shown.

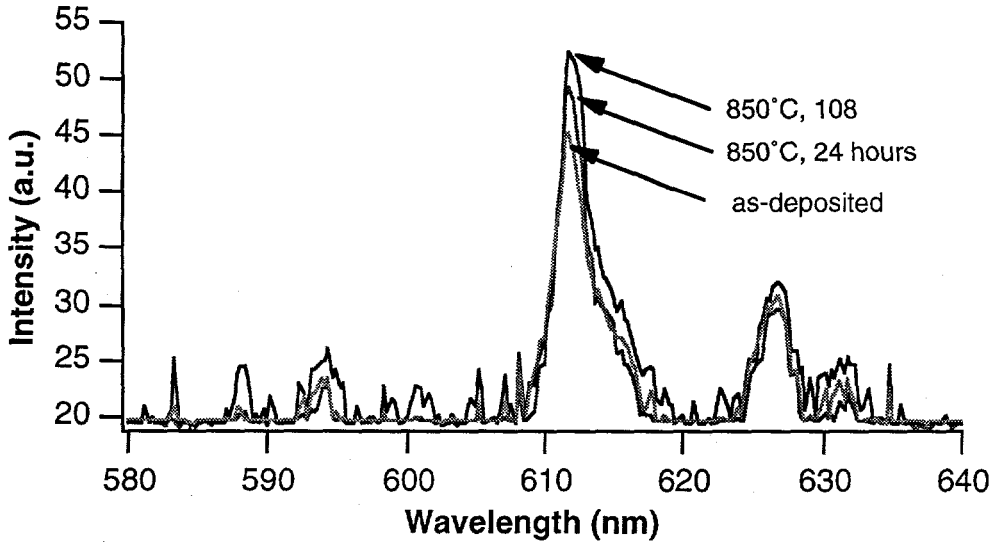

Figure 13 PL spectra of $Y_2O_3:Eu^{3+}$ films deposited for eight hours at 600°C and annealed at 850°C for 24 and 108 hours.